ACADEMIA ROMÂNĂ
*Revue Roumaine de Chimie*
http://web.icf.ro/rrch/

*Rev. Roum. Chim.*,
**2015**, *60*(10), 957-963

# PERFORMANCE EVALUATION OF NATURAL BENTONITE LOADED WITH ZINC OXIDE FOR THE PHOTOCATALYTIC DEGRADATION OF METHYL RED

Mohamad KASSEM

Atomic Energy Commission of Syria, Chemistry Department P.O.Box 6091-Damascus, Syria

*Received May 4, 2015*

Employment of natural clays and their composites, in the catalytic reactions for the disposal of organic pollutants such as dyes, is one of the most fundamental objectives for many researches. In this intention, the present work focused on using the natural Syrian bentonite loaded with different quantity of zinc oxide, as catalysts, for the photodegradation of methyl red. This work has also highlighted the relationship between the structural and textural changes, induced by alteration the amounts of zinc oxide, and the photocatalytic degradation rate for this dye. Impregnation method was used to prepare the composite materials (ZnO- bentonite) according to the weight ratios ZnO/ Bentonite = 0, 0.2, 0.4, 0.6, 0.8, and 1. The prepared samples were characterized using X-ray powder diffraction (XRD), Fourier transform infrared (FT-IR), Differential Thermal Analysis (DTA), nitrogen adsorption apparatus, and UV-Vis spectrophotometer. The experimental results showed that the amount of zinc oxide have influenced the textural and structural characteristics of the bentonite. The results indicated that small amounts of zinc oxide (weight ratios less than 0.4) enhanced the photo degradation of methyl red from 10% to about 55% while the increase in weight ratios (more than 0.4) has a negative effect.

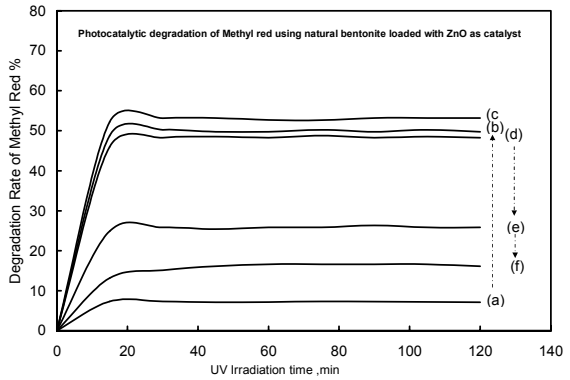


## INTRODUCTION

Increased quantities of organic pollutants resulting from the rapid industrial development have promoted many scientists to seriously search for an effective and economical ways to eradicate these materials which have a large gravity on living organisms in general, and on human health in particular. For this objective, different methods were used to deal with the pollution, including the use of ultraviolet light by exposing contaminated water to these rays in the presence of certain catalysts which led to the disintegration of pollutants to harmless compounds, or to water and carbon dioxide.[1-5] Transition metal oxides such as $TiO_2$, ZnO, $ZrO_2$, $SnO_2$, $MnO_2$, etc. played an important role in this area through the good photocatalysis efficiency, high chemical stability, and low solubility in aqueous solutions. The catalytic activity of these oxides was reinforced when they were supported on a suitable material such as natural clays which have a high specific surface area as well as they are largely available and low cost. So the use of natural clays, loaded with transition metal oxides, for the catalytic reactions has drawn the attention of many

*Corresponding author: cscientific@aec.org.sy

researchers.[6-10] Zinc oxide is one of the most used materials; it is a wide band gap (3.37 eV) semiconductor, abundant, not hazardous, and not costly.[11, 12]

Several researches were carried out on the ZnO/clay composites (e.g. ZnO/montmrillonite), with a view to be used in photocatalytic process such as the degradation of hazardous organic pollutants.[13-20] Very few reports, to our knowledge, have touched on using this type of materials in the photocatalytic degradation of methyl red, which belongs to the dyes group, that have significant damage to the environment and human health. Thus in this work we tried to explore the photocatalytic degradation of methyl red using ZnO/clay materials and chose for this purpose the Syrian bentonite loaded with different quantities of zinc oxide. We also tried in this work to highlight the effect of the amount of zinc oxide on the structural and textural properties of the used bentonite and the relationship between the occurred changes and the degradation rate of methyl red.

## EXPERIMENTAL

### Preparation of materials

The natural bentonite used in this work has been sampled from Rakka province in the north-east of Syria. This clay is composed mainly of montmorillonite and palygorskite as well as a number of other minerals, such as, quartz and dolomite.[21]

ZnO-bentonite composites were prepared by impregnation method according to the weight ratios ZnO/ Bentonite = 0, 0.2, 0.4, 0.6, 0.8, and 1 (weight ratio is the proportionality between the added mass of zinc oxide and a constant mass of bentonite). The mass of untreated bentonite powder was suspended, at room temperature with stirring for 6 h, in an appropriate quantity of zinc acetate solution which was prepared by adding zinc (II) acetate into a mixed solution of propanol and distilled water then, stirring the resultant solution vigorously at 50°C for an hour. The solid phase was kept 24 hours to settle, recovered by centrifugation, washed repeatedly with ethanol, dried in air at 100°C, ground, and finally sintered at 300°C for 3 h.

### Characterization methods

Structural characterizations of the prepared samples were carried out by XRD technique using a STOE STADI P transmission diffractometer, with $CuK_\alpha$ ($\lambda$=0.154049nm) and a linear PSD detector, operated at 50kV and 30mA. All patterns were measured between 5-90 degrees 2θ, with a step size of 0.02 degree.

The quantitative phase analysis was performed using WinXpow 32 Software, which is based on the reference intensity ratio method (RIR) and stored I/Icor values for identifying phase.[22] Absorption bands were also recorded between 400 and 4000 $cm^{-1}$ by a Fourier transform infrared (FT-IR) spectrometer in the transmittance mode (Bruker IFS66). All spectra were obtained at room temperature, using KBr discs containing 0.001g of the material to be studied.

Adsorption-desorption isotherms were performed by BET method[23] at liquid nitrogen temperature using an automated surface area and pore structure analyzer (Quantachrome NOVA2200). The instrument was calibrated using a standard reference material of $Al_2O_3$. Prior to analysis, 0.15-0.2 g of samples was degassed at 100°C for at least 4 hours under vacuum ($10^{-3}$torr). The pore diameter distribution was determined using BJH method.[24]

The DTA measurements of the prepared samples were performed in air at temperature ranging between 20 and 900°C using a Shimadzu DT 40 thermal analyzer with heating rate of 10°C / min.

Diffuse reflectance ultraviolet–visible measurement were performed, at room temperature in the range of 200 to 800 nm, using AvaSpec-2028 fiber optic spectrometer.

The Photocatalytic activity was investigated via degradation of methyl red in aqueous solution under UV irradiation with the presence of natural Syrian bentonite or its composites with ZnO. Inside a 250 ml glass cell, 200 mg of the concerned material was suspended in 200 ml methyl red aqueous solution (30 mg/L). The suspension was irradiated, at room temperature with constant stirring, using a commercial 20W UV lamp as a light source. In each run, the concentration of the methyl red in the solution was measured five times per hour, at $\lambda_{max}$ = 506 nm, using UV-Spectrophometer (UV-3101 PC). The degradation rate was calculated using the formula: (Degradation rate (%) = $[(C_0-C)/C_0] \times 100) \approx [(A_0-A)/A_0] \times 100)$

Where $C_0$ is the initial concentration of methyl red, C the concentration at time *t*, $A_0$ is the initial absorbance and A is the absorbance at time *t*.

## RESULTS AND DISCUSSION

### X-Ray diffraction

Based on the experimental diffraction patterns and using the reference intensity ratio method (RIR) the mineral composition of the natural bentonite was calculated as the following: 33% Montmorillonite (PDF ICDD 3-15), 29% Palygorskite (PDF ICDD 20-688), 18% Quartz (PDF ICDD 5-490), and 19% Dolomite (PDF ICDD 73-1687).

Through a comprehensive look at the X-ray diffraction patterns (Fig. 1), which have been collected for bentonite samples (natural and loaded with different amounts of zinc oxide according to the weight ratios ZnO/Bentonite = 0, 0.2, 0.4, 0.6, 0.8, and 1), one can discern that the addition of zinc oxide may have led to some changes in the structure of the montmorillonite as evidenced by the shift towards low angles of diffraction lines related to this clay mineral. The palygorskite and other components of the bentonite remain unchanged.

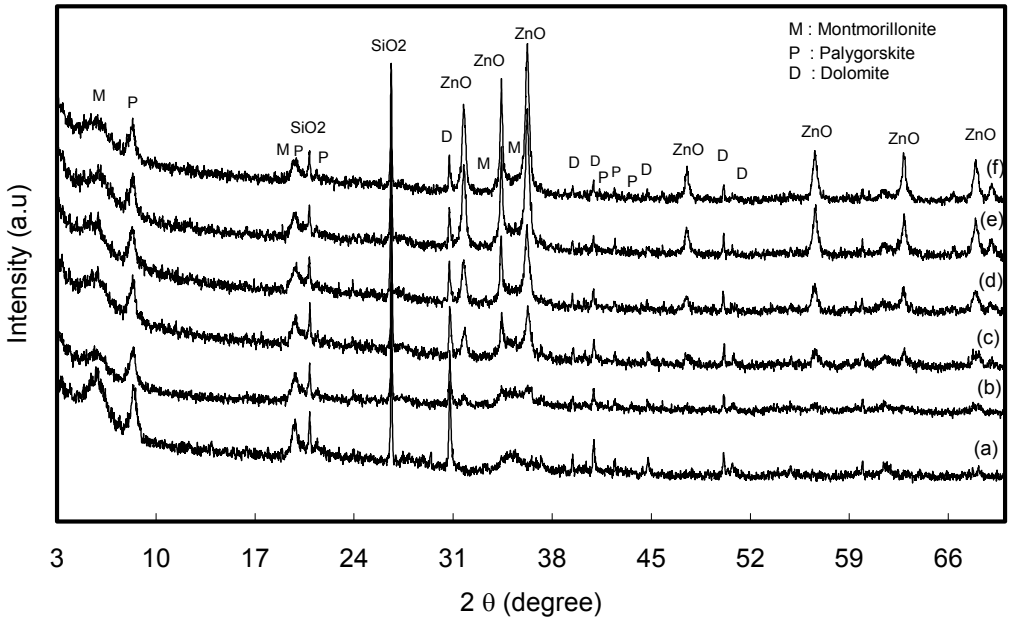


Fig. 1 – X-Ray diffraction patterns of raw bentonite (a)
and samples contain different weight ratio ZnO/bentonite of 0.2 (b) 0.4 (c) 0.6 (d) 0.8 (e) and 1(f).

The montmorillonite mineral becomes less crystalline in the presence of high concentrations of zinc oxide which could be interpreted as a result of an incomplete formation of pillared structure. The unused parts of zinc oxide were dispersed on the surface of the clay where an emergence of diffraction lines related to this oxide was observed in the XRD pattern. These results are in good agreement with those obtained in other research works.[16] Based on the diffraction lines related to ZnO, which is getting intense by increasing the weight ratio, the particle size has been calculated using Scherre equation. It was found that this size has changed from 31.5 nm (for sample with weight ratio = 0.4) to 24.7 nm (for sample with weight ratio = 1).

### Fourier transform infrared (FT-IR)

For supporting the results obtained by XRD, Fourier Transform Infrared spectroscopy FT-IR was used. The recorded spectra (Fig. 2) revealed that the FT-IR spectrum of the pristine bentonite consists of various bands as following: 474cm$^{-1}$ (Si-O-Al), 523cm$^{-1}$ (Si-O-Mg(Fe)), 647cm$^{-1}$ (twisting vibration of Al-OH, Si-O and stretching vibration of Al-O), 924 cm$^{-1}$ (Al-Al-OH deformations), 1000cm$^{-1}$ (Si-O-Si), 1040 cm$^{-1}$ (Si-O), 1660 cm$^{-1}$ (absorbed water), 3440 cm$^{-1}$ (vibration of OH in Al-Mg-OH, Fe-Mg-OH, and Fe-Fe-OH group), 3560 cm$^{-1}$ (corresponds to vibrations of water blocked in palygorskite channels), 3600 cm$^{-1}$ (corresponds to OH stretching vibrations in M-OH group (where M is $Al^{+3}$ or other trivalent cations) 3630 cm$^{-1}$ (Si-OH-Al).[25-28]

When the weight ratio increases, a change in intensities and positions of the bands related to montmorillonite occurs in synchronization with the emergence of new bands located at 1440, 1470, 1570 cm$^{-1}$. Growth of these bands could be attributed to the formation of low concentrations of unidentified compounds formed between zinc oxide and one of the components composing the natural bentonite without being detected by XRD. The lessening of band intensity at 474 and 523 cm$^{-1}$ could be attributed to the destruction of Si-O-Al, Si-O-Mg (Fe) bands, liberation of Mg, Al, Fe ions from octahedral positions in montmorillonite structure and formation of $SiO_2$.[29] The bands of free ZnO were not seen in FT-IR spectra because of overlapping with bands due to Si-O-Si related to bentonite appeared at 523 and 474 cm$^{-1}$.

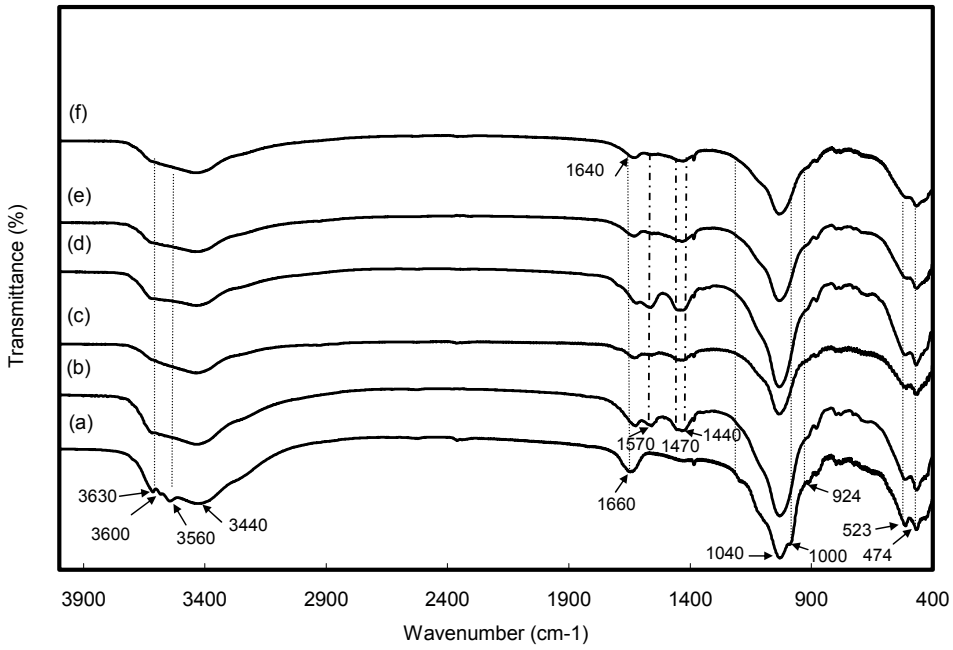


Fig. 2 – FTIR spectra of raw bentonite (a)
and samples contain different weight ratio ZnO/bentonite of 0.2 (b) 0.4 (c) 0.6(d) 0.8 (e) and 1 (f).

## Differential Thermal Analysis (DTA)

The extrapolation of the experimental DTA curves for the studied samples (Fig. 3) disclosed that the endothermic lines between 30 and 145°C are related to the dehydration process. The endothermic line at 240°C of the DTA curves could be related to the removal of interlayer water. The exothermic line at 410°C is related to the decomposition of organic maters incorporated in the clay and/or to the phase transition of the quartz included in the samples. The mentioned line gradually becomes smaller and broader with increasing the weight ratio. Moreover it moves toward the lower temperatures. This difference in the decomposition temperature may be due to the difference in the opening up of the clay layer which restricts the decomposition of the complex. The endothermic lines in the temperatures range 465 – 570°C are related to the dehdroxilation process.

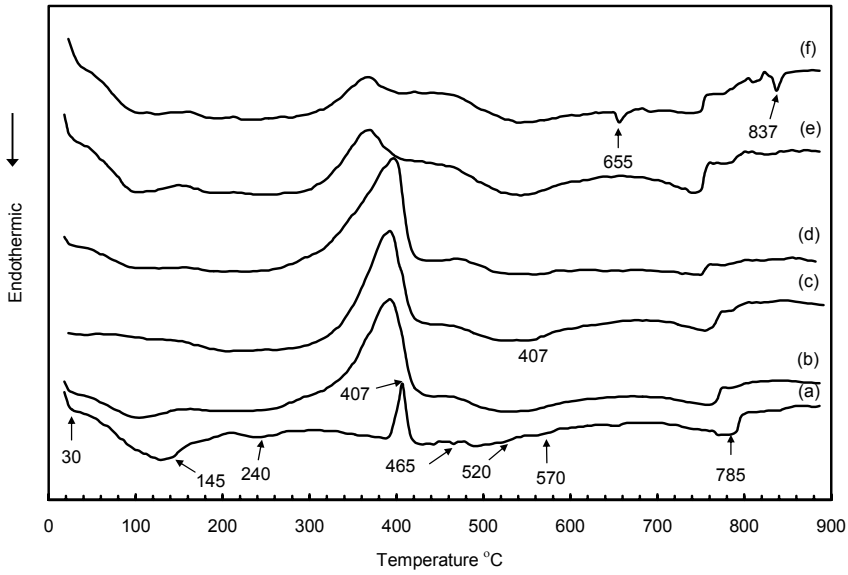


Fig. 3 – DTA curves of raw bentonite (a)
and samples contain different weight ratio ZnO/bentonite of 0.2 (b) 0.4 (c) 0.6(d) 0.8 (e) and 1 (f).

For the endothermic line at 785°C it could be attributed to the decomposition of dolomite impurities.[30-33] When the weight ratio exceeds 0.4, other endothermic lines at 655°C and 837°C start to show up which could be attributed to the formation of unidentified phases ensuing from the reaction between ZnO and the by-products of the solid minerals destruction process.

## Nitrogen adsorption-desorption measurements

The nitrogen adsorption-desorption measurements performed at (-196°C) for all examined samples (Fig. 4) demonstrated that textural characterizations of the used samples varied according to the quantity of added ZnO. The nitrogen adsorption-desorption isotherm related to the natural bentonite Fig.4(*1*), which displays the relationship between the amount of adsorbed nitrogen and relative pressure, follows the type IV which is, according to the classification IUPAC, representative to the mesoporous materials.[34] The hysteresis loop curves resulting from the measurements of the nitrogen adsorption for all samples under study were Similar to the H4 type indicative of the narrow slit-like pores. The pore-size distributions, calculated using BJH method depending on the above mentioned isotherms, revealed that the pore diameters related to natural bentonite sample were centred at 4.5 nm. The incorporation of ZnO causes a broadening and shifting of the distribution line toward the higher pore diameter (about 8 nm) which indicate the enhancement of the mesoporosity of the samples.

Despite the increase in pore size with increasing the amount of zinc oxide, the surface area of the studied samples had declined (Table 1), which refers to the existence of a partial blockage of the pores.

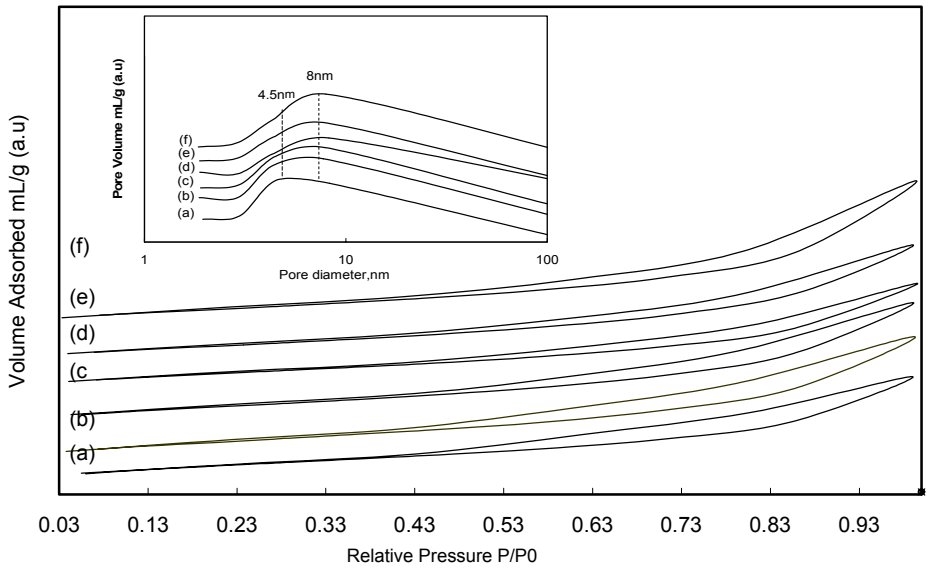


Fig. 4 – Nitrogen adsorption-desorption isotherms and pore size distributions of raw bentonite (a) and samples contain different weight ratio ZnO/bentonite of 0.2 (b) 0.4 (c) 0.6(d) 0.8 (e) and 1 (f).

*Table 1*

Textural properties derived from nitrogen physisorption measurement and band gap values, obtained from DRUV-vis measurements, for ZnO/bentonite samples

| Weight ratio ZnO/Raw bentonite | specific BET surface area ($m^2 g^{-1}$) | Total pore volume ($cm^3 g^{-1}$) | Avarage pore radius (nm) | Band gap energy (eV) |
|---|---|---|---|---|
| 0 | 40.8 | 0.075 | 3.55 | 3.50 |
| 0.2 | 40.6 | 0.085 | 4.00 | 3.06 |
| 0.4 | 40.0 | 0.083 | 4.06 | 3.02 |
| 0.6 | 38.6 | 0.082 | 4.15 | 3.12 |
| 0.8 | 37.9 | 0.072 | 4.16 | 3.15 |
| 1 | 38.0 | 0.071 | 4.34 | 3.20 |

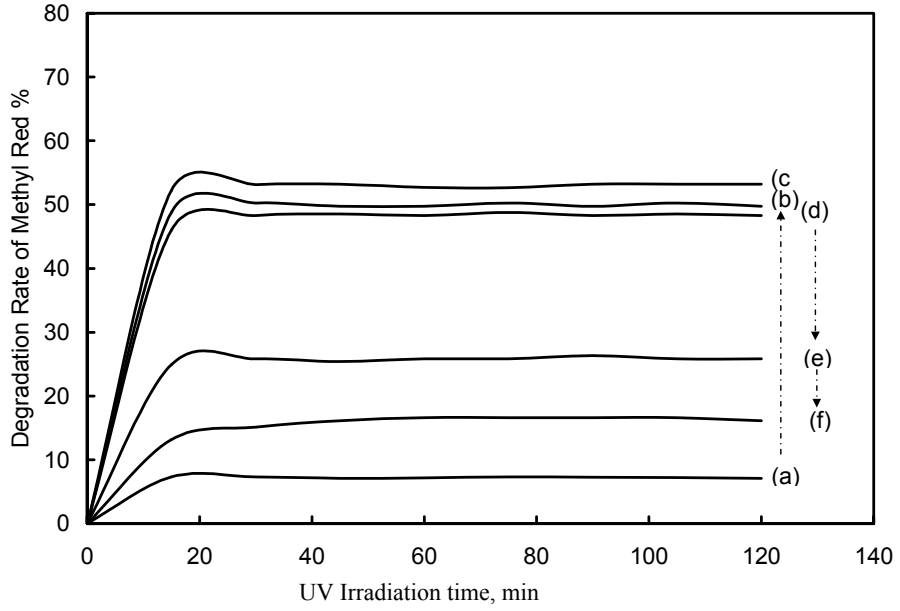


Fig. 5 – Photocatalytic degradation rate of raw bentonite (a)
and samples contain different weight ratio ZnO/bentonite of 0.2 (b) 0.4 (c) 0.6(d) 0.8 (e) and 1 (f).

### Photocatalytic property

The experimental curves representing the degradation rate of methyl red solution versus UV irradiation time with the presence of natural bentonite or those loaded with different amounts of ZnO (Fig. 5) have pointed out a remarkable increase in the degradation rate of methyl red from about 10%, when the natural bentonite was used, to about 50 and 55% in the case of samples containing weight ratios 0.2 and 0.4 respectively. After that, the degradation rate of methyl red decreases gradually with the amount of zinc oxide for up to 15% in the case of the samples containing a weight ratio equal to 1. These changes in catalytic activity could be attributed to several factors: First, and most important, the alteration of the band gap (see Table 1). The second is the difference in the surface area and pore diameter of the studied samples. Moreover, non crystalline materials, may be formed due to the interaction between zinc oxide and some of bentonite components (montmorillonite, palygorskite, quartz and dolomite), this could have a role in preventing the photocatalytic activity of the samples containing high weight ratios. It seems that the zinc oxide, non-intercalated inside the bentonite structure, does not have an effective role in the promotion of the photocatalytic activity even if it has a nanoscale structure.

## CONCLUSIONS

Within the idea of using the clay minerals and their composites in order to obtain catalysts for the treatment of organic contaminants such as dyes in the aqueous solutions; the Syrian bentonite loaded with zinc oxide has shown an acceptable efficiency for the photocatalytic degradation of methyl red.

The results revealed an influence of the ZnO quantity on the textural features of the used bentonite which in turn affected the degradation rate of the aqueous solutions of methyl red under UV irradiation. An increase in the degradation rate occurred from about 10%, in case the use of natural bentonite, to about 55% in the case of samples containing weight ratios ZnO/ bentonite up to 0.4. The degradation rate decrease to less than 15% when the weight ratio is greater than 0.4.

Alteration of the zinc oxide quantity, with impact observed on the textural features of the Syrian bentonite and thus the degradation rate of methyl red, may have also provoked a change in the electronic properties of this clay such as the band gap which is a key parameter in the catalytic activity of the materials. This is what will be investigated in our future work.

*Acknowledgements:* The author would like to thank Professor I. Othman, Director General as well as Dr. Z. Ajji, Head of the Chemistry Department for their encouragement. Thanks are also to Mr. H. Harmalani and Mr. J. Abuhilal for the technical help.

## REFERENCES


1. M. B. Akin and M. Oner, *Ceram. Int*., **2013**, **39**, 9759-9762.
2. T. K. Ghorai, S. K. Biswas and P. Pramanik, *Appl. Surf. Sci*., **2008**, *254*, 7498-7504.
3. C. K. Lee, S. S. Liu, L. C. Juang, C. C. Wang, K. S. Lin and M. D. Lyu, *J. Hazard. Mater.*, **2007**, *147*, 997-1005.
4. Z. Suna, Y. Chen, Q. Ke, Y. Yang and J. Yuan, *J. Photochem. Photobiol.*, *A*, **2002**, *149*, 169-174.
5. P. Tabasom, K. Namratha, I. Ahmed, P. Sukhon and B. Kullaiah, *Int. J.Photoenergy*, **2012**, *Special section*, 1-8.
6. N. Divyal, A. Bansal and AK. Jana, *Bull.Chem.React. Eng.Catal*, **2009**, *4*, 43-53.
7. E. Dvininov, E. Popovici, R. Pode, L. Cocheci, P. Barvinschi and V. Nica, *J. Hazard. Mater.*, **2009**, *167*, 1050-1056.
8. X. Gao and J. Xu, *Appl. Clay Sci.*, **2006**, *33*, 1-6.
9. L. Kőrösi, J. Nemeth and I. Dekany, *Appl. Clay Sci.*, **2004**, *27*, 29-40.
10. C. H. Manoratne, R. M. G. Rajapakse and M. A. K .L. Dissanayake, *Int. J. Electrochem. Sci.*, **2006**, *1*, 32-46.
11. K. Saravanakumar, C. Gopinathan, K. Mahalakshmi, V. Ganesan, V. Sathe and C. Sanjeeviraja, *Adv. Studies Theor. Phys.*, **2011**, *5*, 155-170.
12. R. Viswanatha, T. G. Venkatesh, C. C. Vidyasagar and Y. A. Nayaka, *Arch. Appl. Sci. Res*, **2012**, *4*, 480-486.
13. S. Meshram, R. Limaye, S. Ghodke, S. Nigam, S. Sonawane and R. Chikate, *Chem. Eng. J.*,**2011**, 172, 1008-1015.
14. I. Fatimah, *Int. J. Chem. Sci.*, **2012**, *10*, 1341-1349.
15. I. Fatimah, *J. Mater. Environ. Sci.*, **2012**, *3*, 983-992.
16. I. Fatimah and T. Huda, *Asian J. Mater. Sci.*, **2012**, *4*, 13-20.
17. I. Fatimah, S. Wang and D. Wulandari, *Appl. Clay Sci*., **2011**, *53*, 553-560.
18. C. Hu, J. Song, Z. You, Z. Luan and W. Li, *Biol Trace Elem Res.*, **2012**, *149*, 190-196.
19. S. G. Hur, T. W. Kim, S.-J. Hwang, S.-H. Hwang, J. H. Yang and J.-H. Choy, *J. Phys. Chem. B*, **2006**, **110**, 1599-1604.
20. L. Neuwirthova, V. Matejka, K. M. Kutlakova and V. Tomasek, *Brno*, *Czech Republic*, *EU*, **2012**, *10*, 23-25.
21. Est. *http://www.geology-sy.org*, *General EST of Geology and Minerals Resources* **2009**.
22. Stoe, *WinXpow 32*. **2008**, Stoe and Cie GmbH: Darmstadt Germany.
23. S. Kenneth, *Colloids Surf.*, *A.*, **2001**, *187*, 3-9.
24. J. C. Groen, L. A. A. Peffer and J. P. Ramirez, *Microporous Mesoporous Mater.*, **2003**, *60*, 1-17.
25. Z. Hubicki, E. Zieba, G. Wojcik and J. Ryczkowski, *Mol.Quantum Acoustics*, **2008**, *29*, 109-114.
26. E. Mendelovici, *Clays Clay Miner.*, **1973**, *21*, l15-119.
27. M. Suárez and E. García-Romero, *Appl. Clay Sci.*, **2006**, *31*, 154-163.
28. M. Vlasova, G. Dominguez-Patiño, N. Kakazey, M. Dominguez-Patiño, D. Juarez-Romero and Y.E. Méndez, *Sci.Sintering*, **2003**, *35*, 155-166.
29. N. Khumchoo, M. Ogawa and N. Khaorapapong, *Formation of Zinc Oxide-Smectite Hybrids*, in *PACCON2011 (Pure and Applied Chemistry International Conference 2011)*, **2011**, Bangkok, Thailand.
30. T. Mishra, K. M. Parida and S. B. Rao, *J. Colloid Interface Sci.*, **1996**, *183*, 176-183.
31. M. Onal, Y. Sarilkaya, T. Alemdaroglu and I. Bozdogan, *Turk. J. Chem.*, **2002**, *26*, 409-416.
32. M. Sakizci, B. E. Alver and E. Yorukogullari, *J. Therm. Anal. Calorim.*, **2009**, *98*, 429-436.
33. A. Tabak, B. Afsin, S. F. Aygun and H. Icbudak, *J. Therm. Anal. Calorim.*, **2005**, *81*, 311-314.
34. K. S. W. Sing, D. H. Everett, R. A. W. Haul, L. Moscou, R. A. Pierotti, J. Rouquerol and T. Sieminiewska, *Pure and Appl. Chem.*, **1985**, *57*, 603-619.